DISASTER SCIENCE AND ENGINEERING

2019 - Volume: 5 Number: 1
Page: 1- 10
Received: 14 Mar 2018 Revised: 30 Sep 2018 Accepted: 27 Nov 2018

2016 KAIKOURA EARTHQUAKE TSUNAMI SIMULATION FROM POINT AND FINITE FAULT SOURCE MODELS

Ergin Ulutaş[1,*], Beran Gürleme[1]

[1]Geophysical Engineering Department, Engineering Faculty, Kocaeli University, Kocaeli, Turkey

ABSTRACT

In this study, The numerical simulations of November 13, 2016 Kaikoura, New Zealand earthquake (M_w: 7.8) have been performed. The earthquake occurred at a depth of 15 km at the transition between the Alpine fault in the South Island and the Kermadec-Tonga subduction zone. The approximation of non-linear long wave equations is performed and adopted to simulate tsunami propagations with an initial displacement of the ocean bottom deformation due to faulting. Co-seismic source models proposed by United States Geological Survey (USGS) are further used to represent the effects of various slip models on tsunami prediction along the coastal regions of New Zealand. The maximum value of the initial heights are calculated as 1.18 and -0.2 meters for uplift and subsidence areas from uniform point source models. However, these maximum values are 1.01 and -0.1 meters from finite-fault source models. We have also compared our simulated tsunami waveforms with the observed tide gauge records. The results show that non-uniform slip models could be more effective in prediction of the tsunami heights compared to uniform slip models where the earthquakes involve complex ruptures as in Kaikoura earthquake.

Keywords: Finite fault, point source, fault parameters, tsunami simulation, tide gauges.

1. INTRODUCTION

On 13 November 2016, Northwest coast of New Zealand's South Island experienced a great earthquake (11:02:56 UTC, epicenter -42.69^0 S, 173.02^0 E, 14 km depth) [1]. This earthquake occurred in the Marlborough Fault system, an intricate network of right lateral strike-slip faults connecting the Alpine fault in the South Island to the Hikurangi subduction zone. This region is a very seismically active region. The distribution of M> 5.0 earthquakes in the region between 1920 and 2017 according to their depths and the fault zones in the region are shown in Figure 1 and Figure 2 respectively. The depths of M> 5.0 earthquakes are from U.S. Geological Survey worldwide catalogues of earthquake distributions. The depths of the earthquakes around New Zealand are increasing in the south-west and north-east direction. This increase indicates that the subduction is in the south-west and north-east. Tsunamis can occur in any ocean. But most of them happen in the Pacific Ocean, triggered by the earthquakes and volcanoes. New Zealand, a south pacific country, has experienced many times tsunamis higher than 5m since 1840 according to the historical records. Some were caused by distant earthquakes, but most by seafloor quakes not far off the coast. A magnitude 7.8 earthquake near Kaikoura in 2016 caused minor tsunami along the east coast of New Zealand where the largest onshore waves were recorded at Goose Bay, south of Kaikoura. This study was aimed to simulate the Kaikoura earthquake, to elucidate the effects of uniform and non-uniform slip models on tsunami generation and compare the simulated waveforms with observed one at Kaikoura.

*Corresponding Author:ergin@kocaeli.edu.tr

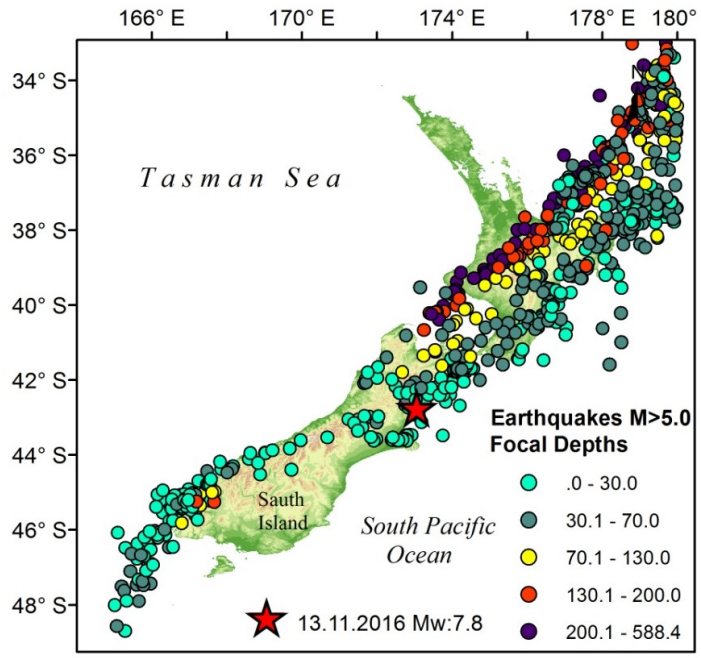

Figure 1. Map of epicenters having the magnitudes larger than M_w:5.0 and focal depths between 0-600 km for the period of 1920-2017.

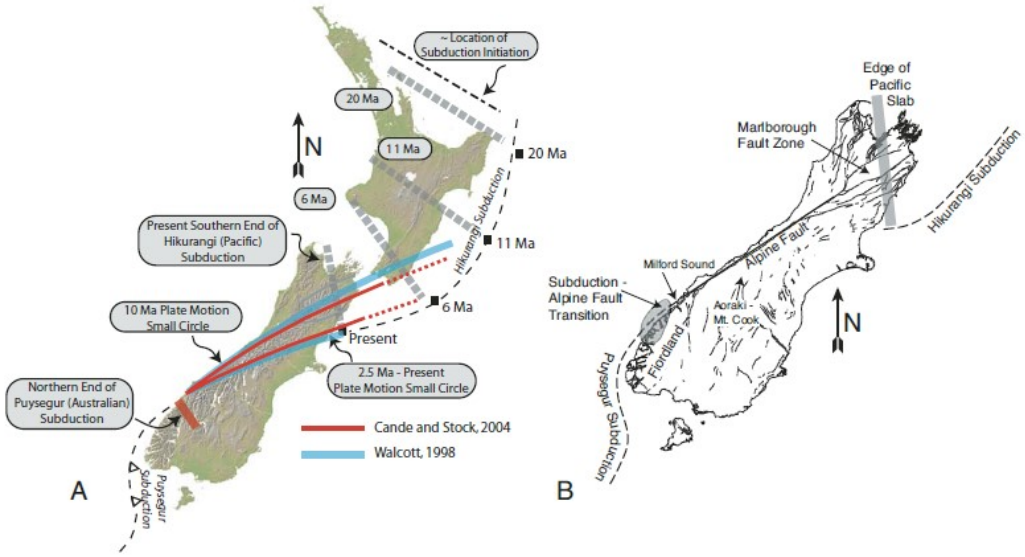

Figure 2. Map showing active faults around New Zealand [2].

2. EARTHQUAKE INDUCED TSUNAMI SOURCE MODELLING

The tsunamis are very large ocean or sea waves that could be triggered by various large-scale deformations of the ocean floor from submarine earthquakes, volcanic activities or landslides. Earthquake-induced tsunamis are very long wavelengths of water and very fast moving waves. They can have wavelengths ranging from 10 to 500 km and periods up to one hour. As a result of their wavelengths, tsunamis act as shallow water waves [3,4]. A wave becomes a shallow-water wave when the wavelength is very large compared to the water depth. Assumptions in calculating the seafloor

deformation define the initial size and height for tsunami propagation. The main factor which determines the initial size and height of a tsunami is the amount of vertical sea floor deformation. In this common approach, it is expected that the initial sea surface displacement mimics the same form as the seafloor displacement (5,6,7,8,9]. Tsunami heights are low on the areas where the tsunamis first formed. As the ripples approach the shore, the water depth decreases and the tsunami heights increase and may lead to the loss of life and property on coastal areas. It is important to determine the size of the deformation of the ocean floor for calculation and propagation of tsunami wave height and arrival times. When an earthquake occurs beneath the sea, the water above the deformed areas of subsidence or uplift with a displacement rate due to earthquake magnitude is displaced from its equilibrium position. Tsunami waves are formed as the displaced water mass, which acts under the influence of gravity, attempts to regain its equilibrium [3,10]. The resulting tsunami wave heights in open sea varies depending on the coastal area batimetry as they approach the shore from open sea.

In this study, the static displacement which is caused by the earthquake is assumed to be equivalent to the first tsunami wave height and this approach was calculated by [11]. This algorithm determines the amount of vertical uplift and subsidence by using the depth, strike, dip and rake of the fault. Then the propagation of the tsunami waves are simulated with the non-linear long wave (shallow water) equations of the fluid flow, using an explicit in time finite difference scheme [12]. The shallow water equations proposed in [13] are implemented into the SWAN code [7]. The set of equations to be solved are:

$$u_t + \frac{1}{\cos(\varphi)} + uu_x + vu_y + \frac{g}{\cos(\varphi)} + \eta_x = fv - \frac{g|U|u}{C^2(D+\eta)} \tag{1}$$

$$v_t + \frac{1}{\cos(\varphi)} + uv_x + vv_y + g\eta_y = -fu - \frac{g|U|v}{C^2(D+\eta)} \tag{2}$$

$$u_t + \frac{1}{\cos(\varphi)} \left\{ \left[(\eta + D)u \right]_x + \left[(\eta + D)v\cos(\varphi) \right]_y \right\} = 0 \tag{3}$$

where φ is the latitude, u and v are the x and y components of the velocity U , g is the gravitational acceleration, t is the time, h is the wave height above the mean water level, f is the Coriolis parameter, C is the coefficient for bottom stress, D is the depth, and indexes refer to partial derivatives.

2.1. Earthquake Parameters

In order to model the tsunami caused by November 13, 2016 (M_w: 7.8) Kaikoura earthquake uniform and non-uniform slip distributions on a single rectangular fault are used. Inıtial tsunami heights are calculated by setting the fault geometry under the assumption of a uniform and non-uniform slip using a statically dislocation model [11] for the input value at the above mentioned Equation 1, Equation 2 and Equation 3. The source parameters for uniform model are from the source parameters of [14] based on the W-phase moment tensor solution (Table 1). The average slip of rectangular fault, fault lengths and width required as inputs for tsunami simulations are calculated by using the empirical relationships proposed by [15] for inverse and thrust faults. Then top of the fault required to be used for the initial heights is calculated as follows :

$$TOF = h - ((\sin\delta)d) \tag{4}$$

where TOF is top of the fault in km, h is the hypocentral depth of earthquake, δ is dip angle and d is the half of fault WFP. It was adopted the hypocentral depth estimates for the initiation of the earthquake is 15.1 km [14]. The hypocenter is assumed at the center of the fault. It should also be note that a centroid location, which is a release point of seismic energy mainly, is not always the same as the hypocenter. Therefore, the hypocentral depths were used instead of centroid depths to define the size of rupture area.

Tablo 1. Source parameters for the tsunami simulation from uniform slip model.

M_w	7.8
Latitude of epicenter	-42.69
Longtitude of epicenter	173.02
Sismik moment	7.040e+20 N-m
Focal depth (km)	15.1
Strike/Dip/Rake	225/36/128
Average slip (m)	3.64
TOF (km)	3.4
Fault Lenght (km)	127
Fault Width (km)	38

The more reliable method to delineate earthquake rupture areas are finite fault model i.e. non-uniform slip models. Non-uniform slip models of fault rupture areas could be constructed through inversion of teleseismic, strong motion, tsunami and geodetic datasets. In this study, the finite fault model of Kaikoura earthquake issued by USGS [16] is used as an input for tsunami simulations as well. Schematic representations of vertical displacement of the seafloor calculated using both uniform and non-uniform models are given in in Figure 3a, b, and cross-sectional representations for both slip models including vertical displacement are given in Figures 4 and Figures 5. By employing uniform and non-uniform slip models, the maximum initial vertical displacements of the ocean bottom are 1.18 in uplift and -0.20 in subsidence for uniform slip model and 1.02 in uplift and -0.10 in subsidence for non-uniform slip model. Although the calculated uplift and subsidence are very close for both slip models, the areas covered by the slip distributions are very different. These difference shows the importance of non-uniform slip models on tsunami simulations.

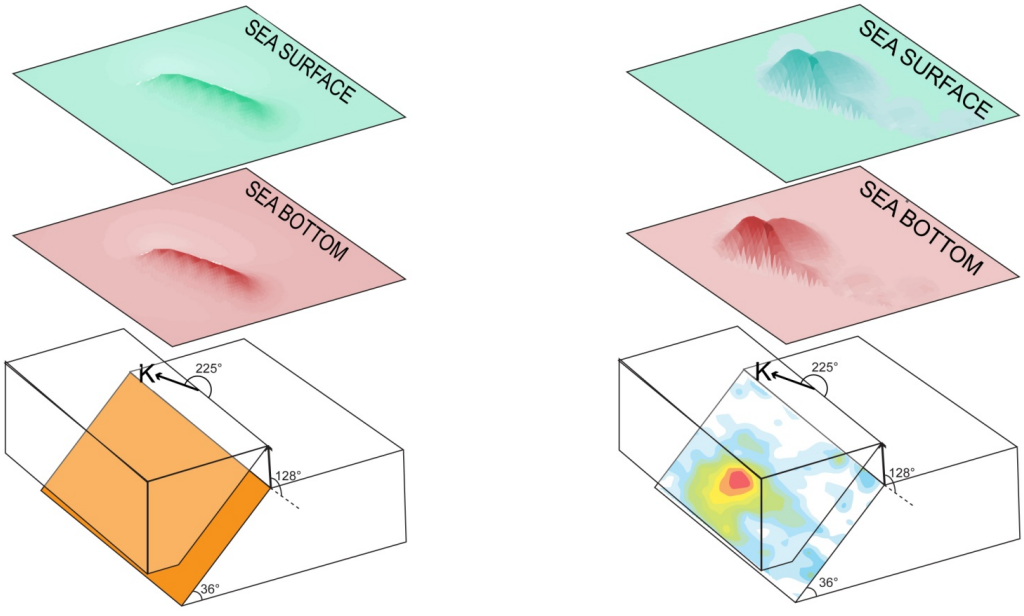

(a) (b)

Figure 3. Schematic representation of vertical displacement of the seafloor calculated from a) uniform slip model, b) non-uniform slip (finite fault) model.

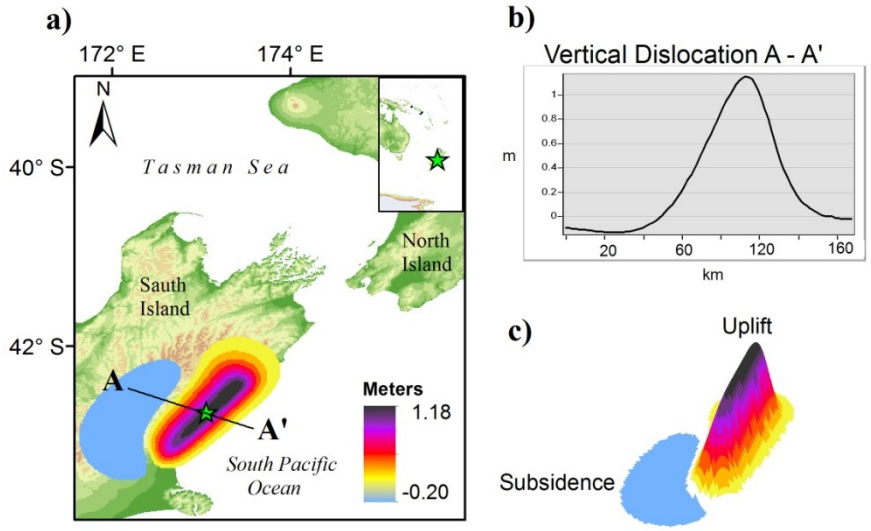

Figure 4. (a) The calculated vertical sea floor dislocation area from uniform faulting, (b), Cross-section of A-A' due to the calculated seafloor deformation, (c) The 3D views of the calculated deformation along the strike of the fault.

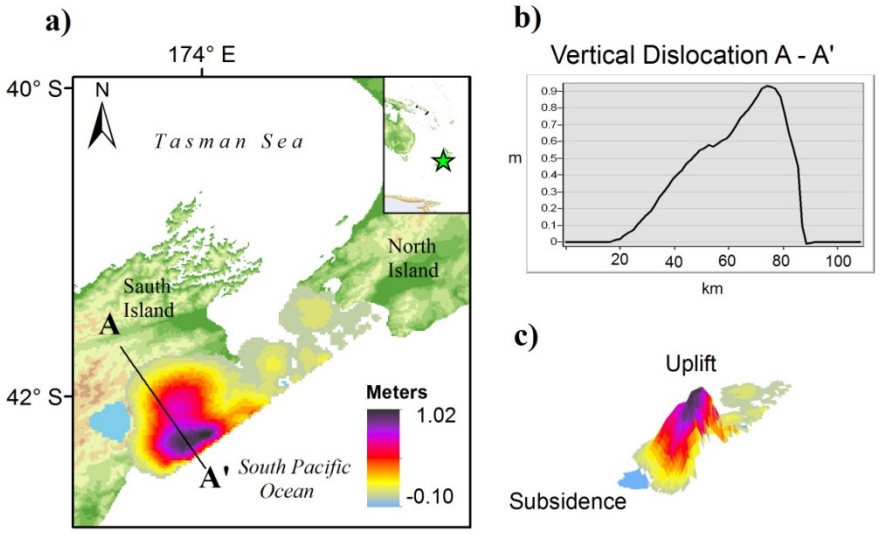

Figure 5. (a) The calculated vertical sea floor dislocation area from non-uniform faulting, (b), Cross-section of A-A' due to the calculated seafloor deformation, (c) The 3D views of the calculated deformation along the strike of the fault.

2.2. Tsunami Simulations

The numerical tsunami simulations by using initial vertical sea floor deformation were performed in geographical coordinates with a GEBCO_08 Grid [17] bathymetric data set. The data set values represent elevation in meters, with negative values for bathymetric depths and positive values for topographic height and the values cover a 30 arc-sec grid of global elevations. The calculation grids consist of 0.5 minutes cell size describing the coastal areas of New Zealand. The calculation times for the tsunami propagations for uniform and non-uniform slip models are both 2.0 hours. The maps of maximum tsunami heights performed using a 0.5 minutes cell size for uniform and non-uniform slip

models are shown in Figure 6 and Figure 7 respectively. The maximum simulated heights are 1.20 m from the uniform slip model and 1.88 from the non-uniform slip model. The maximum calculated heights, when comparing to National Geophysical Data Center (NGDC) maximum heights [18] are reasonable for non-uniform slip model due to the use of inversion source models. The maximum simulated heights from uniform slip models are estimated lower than observed in the region. This lower value is from the elastic deformation theory for modeling the sea floor deformation where the earth is assumed to follow the laws of the classical linear elastic theory which treats it as a homogeneous, isotropic, and elastic material. However, the finite fault models are based on inversion algorithms where the slip distributions are not the same along the fault rupture plane. For that reason, tsunami wave height estimations calculated from non-uniform models could give better results than uniform models. Although it was confirmed that the simulated tsunami heights were over or underestimated from uniform slip models, the advantage of the uniform model approaches is the simplicity and speed of use due to the limited knowledge of the earthquake parameters [4].

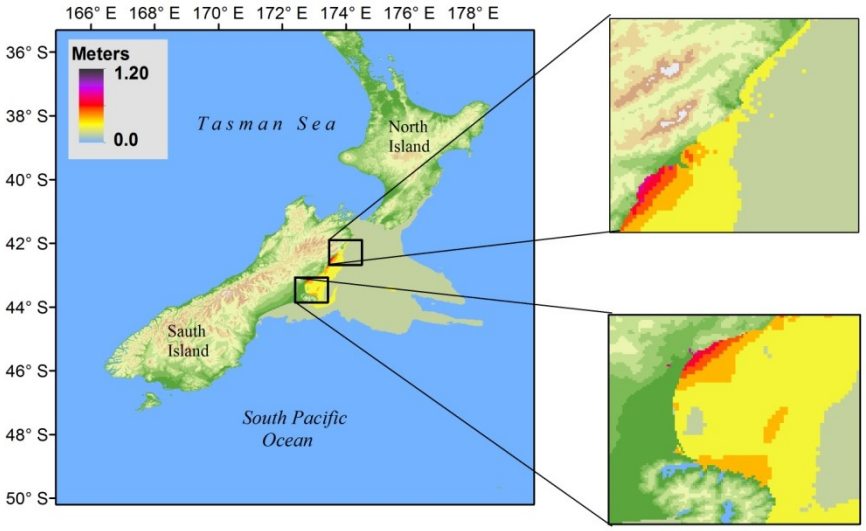

Figure 6. Maximum simulated heights from uniform slip (finite fault) model.

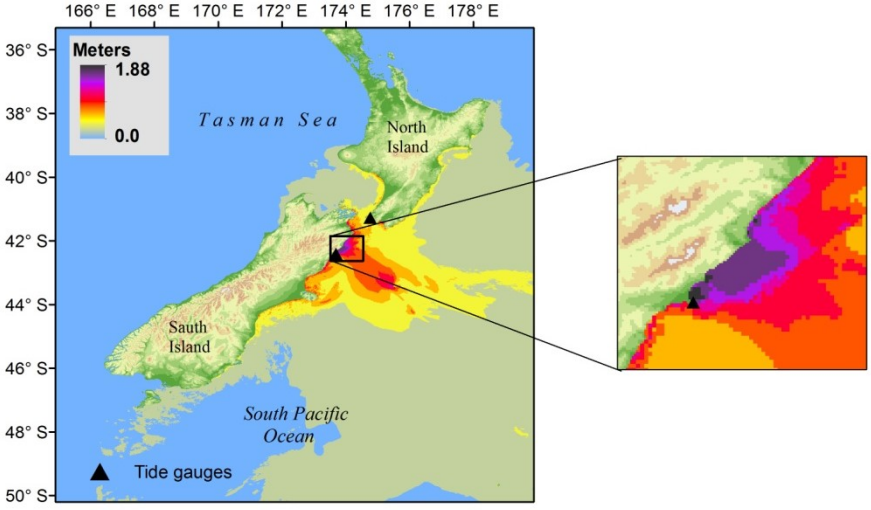

Figure 7. Maximum simulated heights from non-uniform slip (finite fault) model.

3. COMPARISONS OF THE SIMULATED WAVES WITH OBSERVATIONS

The tsunami arrival times and heights are compared with the tsunami records measured at the Kaikoura tide station where the highest wave is recorded (Figure 8 and Figure 9). Tsunami Analysis Tool (TAT) developed by [7] were used to visualize and compare tsunami propagation, tsunami travel time and maximum heights with the records of wave gauges. TAT allows download available sea level measurements from Intergovernmental Oceanographic Commission (IOC) web sources [10, 19]. In order to make the comparisons, the long period noise from the tides due to gravitational effects of the mood and the short period noise from the sea waves due to wind are removed from tide gauges records where the gauges installed along coastal areas. To filter these noise effects on tide gauge records, two days records are examined before the beginning of tsunami wave and a polynomial function at fourth degree is calculated with a script of MATLAB. Then the estimated polynomial function is extracted from the whole record and the filtered tsunami waveform is obtained. At the next stage, Fourier transformations were made in order to manage the frequency band of high and low pass of the record for eliminating the wind waves on tsunami records. By comparing the waveforms for the uniform and non-uniform slip models, estimated waves from uniform model provides lower amplitudes compared to the records of Kaikoura tide gauge (Figure 8). However the arrival time and periods of the waves are in good agreement with the records of Kaikoura from non-uniform slip model. Although the amplitudes of the waves are lower in comparison for non-uniform slip model, the peaks of the are in reasonable time scale with observed ones. These lower amplitudes might be from submarine canyons, channels and narrow embayment that are not well integrated by the 30 arc-sec grid bathymetry data, and thus the underestimated waves are obtained in simulations. Synthetic waves also do not match very well with the trailing waves of tide gauges that exhibit negative and similar periodic waves for all waveform. The estimated maximum wave heights with bar chart visualization in several populated locations around South and North Islands of New Zealand are plotted in Figure 10. The tsunami waves of the earthquake are only affected local area around Kaikoura by producing high amplitude (~ 2 m) tsunami waves far from the epicenter.

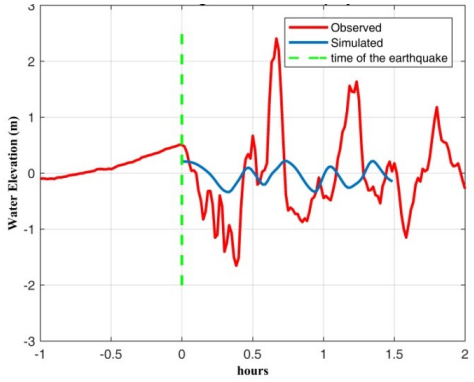

Figure 8. Comparison of the simulated tsunami wave elevation from uniform slip model with observed record at Kaikoura tide gauge station.

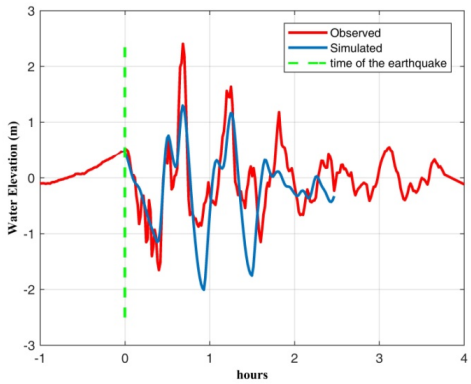

Figure 9. Comparison of the simulated tsunami wave elevation from non-uniform slip model with observed record at Kaikoura tide gauge station.

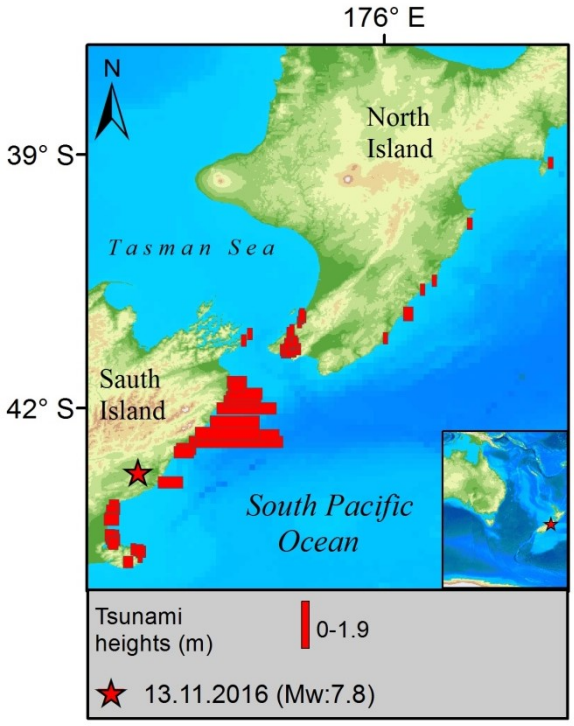

Figure 10. Estimated maximum tsunami wave heights with bar chart visualition in several populated locations in South and North Island of New Zealand.

4. CONCLUSIONS AND DISCUSSIONS

In this study, tsunami simulation of November 13, 2016 (Mw: 7.8) Kaikoura earthquake was performed for uniform and non-uniform slip models. According to the uniform slip model, which is assumed by point source, the initial wave height is calculated as 1.02 m at uplift and -0.20 at subsidence. For the finite fault model (homogeneous slip), the initial height calculated as 1.01 at uplift and -0.10 at subsidence. Despite the higher initial wave is calculated in the uniform slip model, it is not estimated very high waves with this model for the shorelines of New Zealand. However two

meters wave height was measured at Kaikoura which is a town on the east coast of the South Island of New Zealand. Our second adapted non-uniform slip model used for tsunami simulations gives 1.9 meter estimated wave height in Kaikoura. On the other hand, the shape of the estimated waveforms of tsunami in Kaikoura from non-uniform slip model is in a good accordance with the instrumentally recorded data compared with the estimated tsunami waveforms from uniform slip model. The reason could be that the length and width of the fault plane anticipated from the scaling laws are not the effective fault areas where the non-uniform largest slip cumulate. Consequently, determination of fault width, length and slip distributions relying on finite fault models lead to estimate more correctly to estimate the tsunami propagations and heights. For that reason, especially the slip distributions, strike, dip and rake along the subfaults are very important for the tsunami simulations and tsunami early warning systems.

ACKNOWLEDGEMENTS

I would like to thank Alessandro Annunziato for sharing Tsunami Analysis Tool (TAT) program visualizing tsunami simulations and comparing the simulations with DART and tide gauge records. Tsunami waves and their interaction with various topographies were numerically modeled using the SWAN code [13]. ArcMap tools [20] were used to prepare initial wave height and tsunami simulation figures.

*This study is prepared from the paper presented at the 4th International Conference on Earthquake Engineering and Seismology, Eskişehir, Turkey (4ICEES)

REFERENCES

[1] United States Geological Survey (USGS) 2016a. Earthquake Hazard Program, Earthquake details, M 7.8 - 54km NNE of Amberley, New Zealand.
https://earthquake.usgs.gov/earthquakes/eventpage/us1000778i#executive/> (accessed in 2016).

[2] Furlong K.P., 2007. Locating the depth extent of the plate boundary along the Alpine Fault zone, New Zealand: Implıcations for patterns of exhumation in the Southern Alps, Geol S AM S,. 434, 1-15.

[3] Ulutas, E., 2011. Tsunami simulation of the October 25, 2010, South Pagai Island, Sumatra earthquake. Int J Physc Sci 6, 459–475.

[4] Ulutas, E., 2013. Comparison of the seafloor displacement from uniform and non-uniform slip models on tsunami simulation of the 2011 Tohoku–Oki earthquake. J Asian Earth Sci, 62, 568-585, doi:10.1016/j.jseaes.2012.11.007.

[5] Piatanesi A, Tinti S, Pagnoni G., 2001. Tsunami waveform inversion by numerical finite-elements Green's functions. Nat Hazard Earth Sys 1, 187-194.

[6] Yalciner A.C, Pelinovsky E, Talipove T, Kurkin A, Kozelkov A, Zaitsev A., 2004. Tsunamis in the Black Sea: comparison of the historical, instrumental, and numerical data. J Geophys Res. 109,C12023.

[7] Annunziato A., 2007. The Tsunamı Assesment Modelling System by the Joint Research Center. Sci. Tsu. Hazards. 26: 70–92.

[8] Yolsal S, Taymaz T, Yalçıner A.C., 2007. Understanding tsunamis, potential source regions and tsunami prone mechanisms in the Eastern Mediterranean. The Geodynamics of the Aegean and Anatolia, Special Publication: Geological Society, London, Special Publications. 291: 201–230.

[9] Lorito S, Tiberti M.M, Basili R, Piatanesi A, Valensis G., 2008. Earthquake-generated tsunamis in the Mediterranean Sea: scenarios of potential threats to Southern Italy. J Geophys Res. 113, B01301. http://dx.doi.org/10.1029/2007JB004943.

[10] Ulutas E, Inan A, Annunziato A., 2012. Web-based tsunami early warning system: a case study of the 2010 Kepulaunan Mentawai earthquake and tsunami. Nat Hazard Earth Sys. 12, 1855–1871. http://dx.doi.org/10.5194/nhess-12-1855-2012.

[11] Okada Y., 1985. Surface deformation due to shear and tensile faults in a half-space. B Seismol Soc Am. 75, 1135–1154.

[12] Mader C., 2001. Modeling the Lisbon Tsunami. Sci. Tsu. Hazards. 19, 93–116.

[13] Mader C., 1988. Numerical Modeling of water waves, University of California Press, Berkeley, California, p.206, 1988.

[14] United States Geological Survey (USGS) 2016a. Earthquake Hazard Program, Moment Tensor, M 7.8 - 54km NNE of Amberley, New Zealand. https://earthquake.usgs.gov/earthquakes/eventpage/us1000778i#moment-tensor (accessed in 2016).

[15] Wells D.L, Coppersmith K.J., 1994. New empirical relationships among magnitude, rupture length, rupture width, rupture area, and surface displacement. B Seismol Soc Am 84 (4), 974-1002.

[16] United States Geological Survey (USGS) 2016a. Earthquake Hazard Program, Preliminary Finitye Fault Results for the November 13, 2016 Mw 7.9 New Zealand. >https://earthquake.usgs.gov/earthquakes/eventpage/us1000778i#finite-fault<, accessed in 2016).

[17] General Bathymetric Chart of the Oceans–British Oceanographic Data Centre (GEBCO–BODC) (2012) https://www.bodc.ac.uk/data/online_delivery/gebco/gebco_08_grid/ (accessed in 2016).

[18] National Geophysical Data Center (NGDC) (2007) Recent and significant tsunami events. http://www.ngdc.noaa.gov/hazard/recenttsunamis.shtml (accessed in 2017).

[19] Annunziato A, Ulutas E, Titov V.V., 2009. Tsunami model study using JRC-SWAN and NOAA-SIFT forecast methods. In: International Symposium on Historical Earthquakes and Conservation of Monuments and Sites in the Eastern Mediterranean Region 500th Anniversary Year of the 1509, Book of Proceedings, Istanbul, pp. 131–141.

[20] ESRI, 2010. ArcGIS Desktop: Release 10. Environmental Systems Research Institute. Redlands, CA.